Canadian Geotechnical Journal
Revue canadienne de géotechnique

Influence of cross-correlation between nominal load and resistance on reliability-based design for simple linear soil-structure limit states

Journal:	*Canadian Geotechnical Journal*
Manuscript ID	cgj-2017-0012.R1
Manuscript Type:	Article
Date Submitted by the Author:	10-May-2017
Complete List of Authors:	Lin, Peiyuan; Queens University/Royal Military College, Civil Engineering Department Bathurst, Richard; Queens University/Royal Military College,
Keyword:	geotechnical soil-structure interaction, reliability-based design, linear limit state, nominal correlation, bias dependency

CGJ-2017-0012R1 revised submission to CGJ (clean) May 2017

Influence of cross-correlation between nominal load and resistance on reliability-based design for simple linear soil-structure limit states

Peiyuan Lin [1]

Richard J. Bathurst [2]

[1] Post-doctoral Research Associate
Department of Civil Engineering
GeoEngineering Center at Queen's-RMC
Royal Military College of Canada
Kingston, ON, K7K 7B4, Canada
Phone: (613) 541-6000 (ext. 6479/6391); E-mail: Peiyuan.Lin@rmc.ca

[2] Professor and Research Director **(Corresponding Author)**
Department of Civil Engineering
GeoEngineering Center at Queen's-RMC
Royal Military College of Canada
Kingston, ON, K7K 7B4, Canada
Phone: (613) 541-6000 (ext. 6479/6391); Email: bathurst-r@rmc.ca

Abstract

Cross-correlations between nominal load and resistance terms in limit state functions for geotechnical soil-structure interaction problems can be expected. A closed-form solution for the reliability index for a simple linear limit state function is used to examine the influence of nominal load and resistance correlations on computed margins of safety. The formulation also includes the contribution of the underlying accuracy of the load and resistance equations (method bias) and bias dependencies with the magnitude of nominal load and resistance values assumed in the limit state design function. Sensitivity analyses and example problems for the external sliding limit state for a cantilever wall and the pullout limit state for internal stability of reinforced soil walls with different soil reinforcement types are presented. Ignoring nominal correlations where they exist is shown to under-estimate the reliability index in some cases and to over-estimate the reliability index in other cases. In the example problems, these differences are shown to exceed one order of magnitude in terms of probability of failure, but in the sensitivity analyses using a wider range of input parameter values the differences can be several orders of magnitude.

Author keywords: Geotechnical soil-structure interaction; reliability-based design; linear limit state; nominal correlation; bias dependency; sliding; pullout.

Introduction

Geotechnical engineers are often faced with simple soil-structure interaction problems in which the same input parameter definitions appear in both load and resistance terms of a limit state function. Examples are gravity retaining wall structures, anchored sheet pile walls, and pullout of soil reinforcing elements in soil nail walls and mechanically stabilized earth (MSE) walls. These limit states are best expressed within a reliability-based design framework including load and resistance factor design (LRFD). A major objective of modern reliability-based design for geotechnical soil-structures is to achieve a consistent margin of safety expressed by reliability index. A number of different approaches are available to meet this objective including Monte Carlo simulation and simple closed-form solutions based on probability theory. The requirements for modern geotechnical reliability-based design are laid out in ISO2394:2015 Annex D (**International Organization for Standardization 2015**). A useful summary of the arguments in favour of geotechnical reliability-based design can be found in the recent paper by **Phoon (2017)**. However, he also warns against the use of overly simplifying assumptions in closed-form solutions for the purpose of expediency. In this paper we address this issue in the context of the treatment of potentially correlated random nominal load and resistance variables that can arise when considering limit states of the type introduced above within a reliability-based design framework using a general closed-form solution proposed by **Bathurst and Javankhoshdel (2017)**.

The influence of correlations between nominal load and resistance values on computed reliability index in structural engineering applications has been noted by **Ang and Tang (1984)**, **Harr (1987)**, **Melchers (1999)**, and **Nowak and Collins (2012)**. **Ang and Tang (1984)** and **Nowak and Collins (2012)** showed that positive correlations between nominal load and resistance terms can increase or decrease the probability of failure up to one order of magnitude, depending on the formulation and linearity of the limit state function, number of load terms, strength of the correlation, and the distribution of load and resistance random variables. **Harr (1987)** showed that differences in probability of failure greater than one order of magnitude were theoretically possible for cases with cross-correlation coefficient ranging from −1 to +1. Nevertheless, these correlations are not usually a concern in structural engineering problems (e.g. **Melcher 1999**). This simplification has been carried over to geotechnical soil-structure interaction problems where reliability theory-based formulations have been used to compute resistance factors for LRFD calibration (e.g. **Withiam et al. 1998; Allen et al. 2005; Paikowsky 2010**).

Nominal load and resistance correlations in limit state functions used for reliability-based design of geotechnical soil-structures occur when the same random variables for soil properties such as strength and unit weight appear in expressions for both nominal load and resistance terms. In this study, the term *nominal correlation* is used to denote this condition. **Bathurst and Javankhoshdel (2017)** showed that positive nominal correlations in simple soil-structure interaction problems can have a large influence on margins of safety expressed by reliability index or probability of failure. The influence of these correlations can be further amplified if *method bias* for the load and resistance terms is also considered in simple limit-state function formulations. Method bias refers to the accuracy of the underlying deterministic expressions for load and resistance and is a function of the accuracy of the underlying model that describes the mechanics of the problem (*model bias*) plus the uncertainty that results from calibration of models that include one or more empirical parameters (**Allen et al. 2005; Bathurst et al. 2008**). **Phoon and Kulhawy (2003, 2005)** defined a similar quantity called *model factor* which was used to quantify the accuracy of pile load capacity equations with respect to measured loads in pile load test databases. **Bathurst and Javankhoshdel (2017)** gave one example that showed that ignoring positive correlations in the closed-form solution for reliability index that included method bias statistics resulted in over-estimation of probability of failure up to three orders of magnitude for the extreme case of positive nominal cross-correlation coefficient equal to +1.

The main objective of this paper is a broader investigation of the influence of nominal correlations on the magnitude of reliability index for simply linear limit state design functions with one load term and one resistance term using a general closed-form equation for reliability index proposed by **Bathurst and Javankhoshdel (2017)**. The approach considers method bias statistics and method bias dependencies with the magnitude of nominal load and resistance values used at time of design. Example geotechnical design problems expressed by simple linear soil-structure limit states are used to demonstrate the computation of nominal cross-correlation coefficients and method bias statistics and their combined impact on calculated reliability index. Ignoring nominal correlations when they exist is shown to under-estimate the reliability index in some cases and to over-estimate the reliability index in other cases. This is of practical interest to engineers if geotechnical soil-structure design is to move towards fully probabilistic assessments of margin of safety (i.e., reliability-based design).

Closed-form solutions for reliability index of simple linear limit state function

The performance function of interest in this investigation has the following form:

$$g = \lambda_R R_n - \lambda_Q Q_n \tag{1}$$

where R_n and Q_n are random nominal resistance and load values, and λ_R and λ_Q are random resistance and load method bias values computed as:

$$\lambda_R = R_m / R_n \tag{2a}$$

$$\lambda_Q = Q_m / Q_n \tag{2b}$$

Quantities R_m and Q_m represent measured (actual) resistance and load values. Method bias values are used to transform nominal values to measured values. Alternatively stated, they are a measure of the accuracy of the load or resistance equation in a limit state function. Method bias is the combined effect of inaccuracy in the underling deterministic model used for nominal load and resistance calculations (i.e., model error) together with errors due to calibration of these models as explained by **Allen et al. (2005)** and **Bathurst et al. (2008)**. For the idealized case of no difference between nominal (predicted) load and resistance values and corresponding measured values, bias values are equal to +1. This is the assumption used for the block-sliding problem that appears later in the paper because bias values are not available in the literature for this limit state. However, bias statistics can be found in the literature for other soil-structure interaction problems such as shallow foundations (e.g., **Tang and Phoon 2017; Tang et al. 2017**), deep foundations (e.g., **Phoon and Kulhawy 2005; Dithinde et al. 2011; Burlon et al. 2014**), and for internal stability limit states for reinforced soil wall structures (e.g., **Bathurst et al. 2012; Lin et al. 2017a, 2017b**). If all bias and nominal values are assumed to be lognormally distributed, then the reliability index (β) for **Equation 1** can be computed as (**Bathurst and Javankhoshdel 2017**):

$$\beta = \frac{\ln\left[\mathrm{OFS}\sqrt{\dfrac{(1+\mathrm{COV}^2_{Q_n})(1+\mathrm{COV}^2_{\lambda_Q})}{(1+\mathrm{COV}^2_{R_n})(1+\mathrm{COV}^2_{\lambda_R})}}\right]}{\sqrt{\ln\left[(1+\mathrm{COV}^2_{R_n})(1+\mathrm{COV}^2_{\lambda_R})(1+\mathrm{COV}^2_{Q_n})(1+\mathrm{COV}^2_{\lambda_Q})(1+\rho_R\mathrm{COV}_{R_n}\mathrm{COV}_{\lambda_R})^2(1+\rho_Q\mathrm{COV}_{Q_n}\mathrm{COV}_{\lambda_Q})^2/(1+\rho_n\mathrm{COV}_{R_n}\mathrm{COV}_{Q_n})^2\right]}} \qquad (3)$$

The notation format adopted here is that μ denotes mean, COV denotes the coefficient of variation (standard deviation/mean) and ρ_R and ρ_Q are cross-correlation coefficients for random variables R_n and λ_R, and Q_n and λ_Q, respectively. When parameters ρ_R and ρ_Q are non-zero then the limit state is understood to have bias dependencies. This means that the accuracy of the underlying deterministic equations that appear in a limit state function vary with the magnitude of the nominal value. Parameter ρ_n is the cross-correlation coefficient between R_n and Q_n. As before, subscript n denotes predicted (nominal) values. The first term in the numerator is the *operational* factor of safety (OFS) (**Bathurst et al. 2011**) computed as:

$$\mathrm{OFS} = \left(\frac{\mu_{\lambda_R}}{\mu_{\lambda_Q}}\right)\mathrm{FS} = \left(\frac{\mu_{\lambda_R} R_n}{\mu_{\lambda_Q} Q_n}\right) = \left(\frac{\mu_{\lambda_R}\mu_{R_n}}{\mu_{\lambda_Q}\mu_{Q_n}}\right) \qquad (4)$$

The operational factor of safety corrects the conventional mean factor of safety (FS) assumed as the ratio of nominal resistance ($R_n = \mu_{R_n}$) and nominal load ($Q_n = \mu_{Q_n}$) to give a "true" mean factor of safety. It is computed by multiplying the FS used at design time by the ratio of mean of resistance bias values and mean of load bias values.

For the special case of perfect models (i.e., $R_m = R_n$, $Q_m = Q_n$) and OFS = FS, **Equation 3** reduces to:

$$\beta = \frac{\ln\left[FS\sqrt{\dfrac{(1+COV_{Q_n}^2)}{(1+COV_{R_n}^2)}}\right]}{\sqrt{\ln\left[\dfrac{(1+COV_{R_n}^2)(1+COV_{Q_n}^2)}{(1+\rho_n COV_{R_n} COV_{Q_n})^2}\right]}} \qquad (5)$$

This equation can be found in the related literature (e.g., **Harr 1987**; **Phoon 2008**). For the case of uncorrelated R_n and Q_n values, $\rho_n = 0$ and **Equation 3** reduces to:

$$\beta = \frac{\ln\left[OFS\sqrt{\dfrac{(1+COV_{Q_n}^2)(1+COV_{\lambda_Q}^2)}{(1+COV_{R_n}^2)(1+COV_{\lambda_R}^2)}}\right]}{\sqrt{\ln\left[(1+COV_{R_n}^2)(1+COV_{\lambda_R}^2)(1+COV_{Q_n}^2)(1+COV_{\lambda_Q}^2)(1+\rho_R COV_{R_n} COV_{\lambda_R})^2(1+\rho_Q COV_{Q_n} COV_{\lambda_Q})^2\right]}} \qquad (6)$$

It should be noted that the log term in the denominators of **Equations 3**, **5** and **6** must be positive in order for the reliability index to be a real value. However, in the limit of the denominator term approaching zero the value of β approaches infinity so design outcomes are safe and this numerical result is not of practical concern. In the next section, a parametric study is first carried out using **Equation 5** to investigate the influence of ρ_n on reliability index; then **Equation 6** is employed to explore the influence of cross-correlation parameters for method bias, ρ_R and ρ_Q on β; and lastly, the combined influence of ρ_n with ρ_R and ρ_Q on β is examined.

Parametric study of the influence of cross-correlation coefficients ρ_n, ρ_R and ρ_Q on reliability index

Influence of cross-correlation coefficient ρ_n for nominal load and resistance terms

The impact of ρ_n on reliability index is investigated for the case of COV of both Q_n and R_n ranging from 0 to 0.50 and FS varying from 1 to 10. The maximum possible limits on the full range of ρ_n are −1 and +1. A negative value of ρ_n indicates that Q_n and R_n are negatively correlated, in which case R_n tends to decrease linearly as Q_n increases, or vice versa. A positive value of ρ_n implies that Q_n and R_n tend to increase or decrease simultaneously. If ρ_n = 0, then Q_n and R_n are statistically linearly independent.

Figure 1 shows plots of reliability index, β, versus factor of safety, FS, for cases with $\rho_n = -1$, −0.5, 0, 0.5 and 0.9 using **Equation 5** with $COV_{Q_n} = COV_{R_n} = 0.20$. Results for $\rho_n = +1$ are not shown because this value with $COV_{Q_n} = COV_{R_n}$ gives zero for the denominator of **Equation 5** and thus infinite β value.

As expected, for the same value of ρ_n, β increases linearly with the log of FS. For a constant value of FS, β increases with ρ_n increasing from −1 to 0.9. This means that ignoring the correlation between nominal load and nominal resistance (i.e., assume nominal cross-correlation $\rho_n = 0$) results in under- and over-estimation of the reliability index if Q_n and R_n are positively and negatively correlated, respectively. For instance, for FS = 2 and $\rho_n = -1$, β = 1.73 (probability of failure P_f = 4.18%) but for the case of $\rho_n = 0$, β = 2.47 (P_f = 0.68%). The difference is close to one order of magnitude in terms of probability of failure. For the case of $\rho_n = 0.9$ the reliability index is very large, i.e. β = 7.90 ($P_f = 1.39\times10^{-15}$). The differences identified here show that the impact of ρ_n on β is much greater when values of ρ_n are positive. The influence of ρ_n on reliability index also increases with magnitude of FS. For example, when FS = 3 the β values are equal to 2.75 (P_f = 0.30%) and 3.92 (P_f = 0.0044%) for $\rho_n = -1$ and 0, respectively. The difference in P_f is roughly two orders of magnitude.

Contour plots of β versus $COV_{Q_n} = COV_{R_n}$ for FS = 2 and $\rho_n = -1$, −0.5, 0, 0.5 and 1 using **Equation 5** are available in **Figure S1** of the **Supplemental Materials** to this paper. One example appears here as **Figure 2** corresponding to positively cross-correlated Q_n and R_n with $\rho_n = 0.5$. The horizontal trajectory of β values drawn at $COV_{Q_n} = 0.20$ gives 3.60, 4.14 and then 3.52 for COV_{R_n} equal to 0, 0.10 and 0.20, respectively. Other trajectories in COV_{Q_n} and COV_{R_n} space in this figure and the companion figures in the **Supplemental Materials** with different cross-correlation coefficients result in a wide range β responses. However, as expected, combinations of lower values of COV_{Q_n} and COV_{R_n}, when all other parameters are kept the same, give higher reliability index values.

Influence of cross-correlation coefficients ρ_R and ρ_Q for method bias and nominal resistance and load values

Bias dependencies between model resistance bias and nominal resistance (ρ_R) have been examined in the literature for different geotechnical soil-structure interaction problems for shallow foundations, deep foundations, and for internal stability limit states for reinforced soil wall structures. The need to consider bias dependency in reliability-based design or LRFD calibration of geotechnical structures has been emphasized by **Phoon and Kulhawy (2003)**, **Phoon (2017), Dithinde et al. (2011), Tang and Phoon (2017) and Tang et al. (2017)**, amongst others. The quantitative influence of ρ_R and ρ_Q on computed reliability index is explored in this section.

Reliability index β computed using **Equation 6** is plotted against operational factor of safety OFS in **Figure 3**. In this figure nominal values of load and resistance are uncorrelated (ρ_n = 0) but load and resistance method bias is correlated with nominal values of load and resistance (i.e., there are bias dependencies). The magnitude of β increases linearly with the log value of the operational factor of safety. However, the slopes of the curves are greater when ρ_R and ρ_Q are both negative. When ρ_R and ρ_Q have opposite signs the difference in β values from the case of $\rho_R = \rho_Q = 0$ is less, because the terms with these parameters in **Equation 6** oppose each other. The consequences of combinations of ρ_R and ρ_Q with different signs on β can be appreciated by following the vertical trajectory of the line drawn at OFS = 2 which shows that β increases in the order of 0.75, 1.01 and 2.71 for $\rho_R = \rho_Q = 1$, 0 and −1, respectively. Finally, the greater the magnitude of OFS, the greater the difference in β values with changes in the magnitude of $\rho_R = \rho_Q$.

The effect of magnitude and sign of ρ_R and ρ_Q on β is explored further in **Figure 4**. For the case of ρ_R and/or ρ_Q increasing from −1 to +1, β decreases. When ρ_R and ρ_Q have the same sign, the influence on β is amplified as indicated by the diagonal line with $\rho_R = \rho_Q$. For ρ_R and ρ_Q with opposite sign, the influence of these terms is partly negated as noted earlier and demonstrated by the diagonal line for $\rho_R = -\rho_Q$.

Figure S2 in the **Supplemental Materials** to this paper shows contour plots of β versus COV_{λ_R} and COV_{λ_Q} for $\rho_R = \rho_Q = -1, -0.5, 0, 1$, $\rho_R = -1$ and $\rho_Q = +1$, and $\rho_R = +1$ and $\rho_Q = -1$. The first of these figures is reproduced here as **Figure 5**. Similar to the trend described for data in **Figure 3**, a horizontal trajectory at $COV_{\lambda_Q} = 0.4$ shows β increasing slightly at first and then decreasing thereafter. The last two plots in **Figure S2** of the **Supplemental Materials** show that when ρ_R and ρ_Q are of opposite sign, β is more sensitive to the magnitude of COV_{λ_Q} for the case of $\rho_R = -1$, and more sensitive to COV_{λ_R} for the case of $\rho_Q = -1$.

Combined influence of nominal cross-correlation ρ_n and bias cross-correlations ρ_R and ρ_Q

Figure 6 shows plots of β versus OFS using **Equation 3** where both bias dependencies (i.e., ρ_R and ρ_Q) and nominal correlation (i.e., ρ_n) are taken into account. The grey shaded regions correspond to β values computed using ρ_R and ρ_Q equal to different combinations of −1 to +1. The upper and lower limits on each region correspond to $\rho_n = +1$ (or +0.6) and −1, respectively. β is very sensitive to ρ_n when ρ_R and ρ_Q are both negative. Consider the case of OFS = 2 with $\rho_R = -1$ and $\rho_Q = -1$; β is equal to 1.75 and 2.71 corresponding to $\rho_n = -1$ and 0, but β = 8.16 for $\rho_n = 0.6$. This is an unfavorable outcome for pullout limit states of reinforcing elements since bias dependencies reported in the literature (e.g., **Huang and Bathurst 2009**; **Yu and Bathurst 2015**; **Allen and Bathurst 2015**; **Lin et al. 2017a, 2017b**) have been shown to always be negative for both load and resistance models. The importance of considering ρ_n in the computation of reliability index using closed-form solutions for these limit states is thus confirmed. For cases where ρ_R and ρ_Q are both positive or of opposite signs, the influence of ρ_n is much less.

The importance of ρ_n is further revealed in **Figure 7** which shows contour plots of β versus $COV_{R_n} = COV_{Q_n}$ and $COV_{\lambda_R} = COV_{\lambda_Q}$ using **Equation 3**. The nominal cross-correlation ρ_n is set to 0.5 and −0.5. Cross-correlation parameters for bias dependencies are $\rho_R = \rho_Q = -0.5$. Reversing the sign of ρ_n results in opposite trends in β. For example, for $\rho_n = -0.5$ and constant $COV_{\lambda_R} = COV_{\lambda_Q} = 0.4$, increasing $COV_{R_n} = COV_{Q_n}$ from 0.2 to 0.6 leads to β decreasing from 2.19 to 1.23 (**Figure 7a**). For the same conditions and $\rho_n = 0.5$ in **Figure 7b**, β increases from 2.65 to 4.17.

The implications of different combinations of nominal cross-correlation parameters and bias dependencies on reliability index are demonstrated in the next section using simple design cases.

Problem examples

Formulation of limit state functions

Two example limit states are investigated here. The first example is the frictional sliding block problem shown in **Figure 8a** with block height (H), length (L), unit weight (γ_R) and base friction angle (ϕ_R). A horizontal active force is assumed to act against the vertical side of the block. This force is a function of the retained soil unit weight (γ_Q) and friction angle (ϕ_Q). A practical example is the block comprising of the facing and reinforced soil zone in an MSE wall that is used to compute the margin of safety against external sliding. The outside dimensions of a concrete cantilever wall including the soil over the heel and toe is another example.

The nominal resistance is computed as:

$$R_n = HL\gamma_R \tan\phi_R \tag{7}$$

and the nominal load as:

$$Q_n = \frac{1}{2}\tan^2\left[\frac{\pi}{4} - \frac{\phi_Q}{2}\right]\gamma_Q H^2 \tag{8}$$

The second example (**Figure 8b**) is the ultimate pullout limit state for a planar soil reinforcement element of anchorage length L_e located at depth z below the backfill surface in the passive zone of a reinforced soil wall with soil unit weight (γ_R) and friction angle (ϕ_R). The pullout resistance is developed in response to the active earth pressure acting against a contributory area of the wall face of height S_v and width S_h. The active earth pressure is a function of depth z to the middle of the contributory area (equal to the reinforcement depth), and properties of the soil in the active zone behind the wall facing (soil unit weight (γ_Q) and friction angle (ϕ_Q)). The reinforcement layer may be continuous or discontinuous in the plane strain direction. If the reinforcement is a geosynthetic sheet (geogrid or geotextile), the nominal resistance is computed as (**FHWA 2009**; **Huang and Bathurst 2009**):

$$R_n = \alpha L_e z \gamma_R \tan\phi_R \tag{9}$$

where α is an empirical interaction coefficient. The nominal load can be expressed as (**FHWA 2009**; **AASHTO 2014**):

$$Q_n = \tan^2\left[\frac{\pi}{4} - \frac{\phi_Q}{2}\right]\gamma_Q z S_v \tag{10}$$

For a MSE wall with steel strip or steel grid reinforcement, the nominal resistance (R_n) and load (Q_n) are computed as (**PWRC 2014**; **FHWA 2009**; **AASHTO 2014**; **Yu and Bathurst 2015**):

$$R_n = 2FL_e wz\gamma_R \tag{11}$$

where F is a dimensionless pullout resistance factor and w is the width of the steel strip or steel grid and

$$Q_n = \kappa \tan^2\left[\frac{\pi}{4} - \frac{\phi_Q}{2}\right]\gamma_Q z S_v S_h \quad (12)$$

Here, κ is a dimensionless pullout resistance factor that is a function of z.

For reinforcing elements comprised of a row of soil nails, the nominal resistance and load are calculated as (**Watkins and Powell 1992**; **GEO 2007**; **FHWA 2015**; **Lin et al. 2017a**):

$$R_n = 2DL_e z \gamma_R \tan\phi_R \quad (13)$$

where D = nail diameter, and

$$Q_n = \eta \tan^2\left[\frac{\pi}{4} - \frac{\phi_Q}{2}\right]\gamma_Q H S_v S_h \quad (14)$$

Here, η = empirical piecewise or continuous function of normalized nail depth (z/H).

Similar expressions can be developed for other types of anchorage systems that rely on the frictional strength of the anchorage zone to develop pullout resistance (e.g., **Miyata et al. 2011**). As before, soil properties are taken as random variables and all other parameters are deterministic.

The focus here is on the influence of the random variables for the soil in resistance and load terms. The general form of these limit state functions (**Equation 1**) is:

$$g = \lambda_R R_n(A, \gamma_R, \tan\phi_R) - \lambda_Q Q_n\left(B, \gamma_Q, \tan^2\left[\frac{\pi}{4} - \frac{\phi_Q}{2}\right]\right) \quad (15a)$$

or

$$g = \lambda_R R_n(A, \gamma_R) - \lambda_Q Q_n\left(B, \gamma_Q, \tan^2\left[\frac{\pi}{4} - \frac{\phi_Q}{2}\right]\right) \quad (15b)$$

The last equation is for the case of the limit state with R_n and Q_n computed using **Equations 11** and **12**. The deterministic parameters identified in the load and resistance equations introduced earlier have been collected together in constant terms A and B.

The random variables in **Equation 15** are λ_R, γ_R, ϕ_R, λ_Q, γ_Q and ϕ_Q. Different design scenarios can be imagined for $\phi_R = \phi_Q = \phi$ and $\gamma_R = \gamma_Q = \gamma$. Here, $\phi_R = \phi_Q = \phi$ means that ϕ_R and ϕ_Q are the same random variable denoted as ϕ. The nominal load Q_n and nominal resistance R_n are cross-correlated. Similarly, this paper uses $\phi_R \neq \phi_Q$ to denote that ϕ_R and ϕ_Q are two independent random variables (i.e., two different populations), although they may have the same statistical parameters (i.e., same mean ($\mu_{\phi_R} = \mu_{\phi_Q}$) and same coefficient of variation ($COV_{\phi_R} = COV_{\phi_Q}$)). The same interpretation applies to $\gamma_R = \gamma_Q = \gamma$ and $\gamma_R \neq \gamma_Q$. Five different cases are summarized in **Table 1**. Each case will yield a different nominal cross-correlation coefficient ρ_n for the four random nominal load and resistance variables as demonstrated in the next section. Maximum and typical ranges for mean and COV of friction angle and unit weight for frictional soils are summarized in **Table 2** based on values reported in the literature (e.g., **Lacasse and Nadim 1996**; **Phoon and Kulhawy 1999**; **Baecher and Christian 2003**). As noted earlier, friction angle and unit weight are assumed to be lognormally distributed.

Computation of cross-correlation coefficient ρ_n for nominal load and resistance variables

In this section, the sliding block problem is considered first using the limit state function expressed by **Equation 15a**. To simplify calculations and to focus on the influence of nominal correlation, correlations between ϕ and γ within each load and resistance equation are ignored. The computation of ρ_n (Pearson's ρ) between nominal load and resistance variables is carried out assuming H = 10 m and L = 6 m. In fact, the magnitude of ρ_n is independent of the magnitude of deterministic parameters that appear in all limit state equations introduced earlier (e.g., see the textbook by **Soong 2004**). Hence, constant terms A and B in **Equation 15a** could be taken as +1 in the Monte Carlo (MC) simulations to follow.

Figure 9a presents a scatter plot of R_n against Q_n from n = 3000 MC realizations for Case 1. In this case the values of ϕ and γ for load and resistance terms are not the same. Hence, during each MC realization a different population of ϕ and a different population of γ are sampled for load and resistance terms. The mean and COV of ϕ and γ values are shown in the figure captions. For convenience these values are the same. As expected there is no visual correlation between R_n and Q_n and this is confirmed quantitatively by the horizontal regressed line through the data points and the computed Pearson's ρ which is 0 to two decimal places.

Figure 9b presents a scatter plot of R_n against Q_n with n = 3000 data points for Case 2 and the same sliding block example with the same input parameters. In this case the values of ϕ and γ in load and resistance terms are the same. Hence, during each MC realization a single population of ϕ and a single population of γ are sampled. These data are highly negatively correlated with $\rho_n = -0.72$

In **Figure 9** the data are plotted for 3000 MC realizations for illustrative purposes (i.e., to see individual data points). However, to increase accuracy of the estimation of ρ_n to two significant figures, all simulations were run out to $n = 10^6$ realizations and these results are used hereafter.

The same general approach described above to compute ρ_n can be used for limit states expressed by **Equations 15a** and **15b**. The influence of COV values of γ_R, ϕ_R, γ_Q and ϕ_Q on computed ρ_n values are investigated next for both equations. The ratio $r = COV_\phi / COV_\gamma = 2$ is the maximum ratio of the COV of ϕ and γ values in **Table 2**. **Figure 10** shows that for these conditions ρ_n remains essentially constant at about 0, –0.70, 0.14, 0.39 and –0.83 for Cases 1, 2, 3, 4 and 5, respectively.

Figure 11 shows the influence of the magnitude of ratio r on ρ_n. For Case 1, all variables are uncorrelated and thus ρ_n remains zero. However, for all other cases the value of ρ_n decreases with increasing magnitude of the ratio of $r = COV_\phi / COV_\gamma$. For Case 2, ρ_n is –0.18 for r = 1 but falls to –0.89 as r increases to 4. The reason is that as r increases, the uncertainty in friction angle (COV_{ϕ} term) contributes more to the uncertainty in both R_n and Q_n while the influence of uncertainty in soil unit weight (COV_{γ} term) is less. This can be appreciated by the form of **Equations 7** and **8** to compute R_n and Q_n which are more sensitive to the magnitude of friction angle ϕ than to unit weight γ. Increasing ϕ values result in increasing R_n and decreasing Q_n values (i.e., increasing negative correlation). The effect is amplified as r becomes larger.

The sensitivity of ρ_n to magnitude of friction angle can be seen in **Figure 12** for cases with one or two correlated soil parameters and the mean of friction angles $\mu_{\phi_R} = \mu_{\phi_Q}$. In contrast, **Figure 13** shows that ρ_n is essentially independent of the means of unit weight, $\mu_{\gamma_R} = \mu_{\gamma_Q}$, over a reasonable range of 14 to 22 kN/m^3. This is due to the appearance of γ_R and γ_Q as linear terms in both expressions for the R_n and Q_n, respectively.

The friction angle of a soil can be expected to vary with unit weight (**Matsuo and Kuroda 1974**; **Parker et al. 2008**). Here, this correlation is denoted by cross-correlation coefficients ρ_{ϕ_R,γ_R} and ρ_{ϕ_Q,γ_Q}, and their influence on ρ_n is shown in **Figure 14** for values in the range from −0.7 to 0.7 and assuming ρ_{ϕ_R,γ_R} and ρ_{ϕ_Q,γ_Q} are equal. Case 1 with uncorrelated variables ($\rho_n = 0$) can be considered as the reference case. Cross-correlation parameters ρ_{ϕ_R,γ_R} and ρ_{ϕ_Q,γ_Q} have little effect on ρ_n for Case 3. Cases 2 and 5 can be seen to be only slightly influenced by the magnitude of cross-correlation between soil friction angle and soil unit weight. In contrast, there is a very strong influence of $\rho_{\phi_R,\gamma_R} = \rho_{\phi_Q,\gamma_Q}$ values on ρ_n for Case 4. For $\rho_{\phi_R,\gamma_R} = \rho_{\phi_Q,\gamma_Q}$ increasing from −0.7 to 0.7, ρ_n decreases from 0.85 to −0.37. The practical range of interest is $\rho_{\phi_R,\gamma_R} = \rho_{\phi_Q,\gamma_Q} > 0$ since the expectation is that friction angle increases with soil unit weight and this is the assumption made in the related literature (e.g., **Chowdhury and Xu 1993**; **Low and Tang 1997**; **Babu and Srivastava 2007**; **Babu and Singh 2011**). As examples, the cross-correlation coefficient between friction angle (degrees) and dry unit weight of cohesionless soil was computed as $\rho_{\phi,\gamma}$ = 0.48 (**NCHRP 2004**). The values of $\rho_{\phi,\gamma}$ were calculated as 0.57 and 0.22 by **Javankhoshdel and Bathurst (2017)** based on measured values of ϕ and γ reported by **Lee and Singh (1968)** and **Stuedlein et al. (2011)**, respectively.

If ρ_{ϕ_R,γ_R} and ρ_{ϕ_Q,γ_Q} are positive, the practical range for ρ_n is from 0.39 to –0.37. For $\rho_{\phi_R,\gamma_R} = \rho_{\phi_Q,\gamma_Q}$ ranging from 0 to 0.40, the ρ_n values are positive; thus ignoring ρ_n leads to underestimation of β and safer design outcomes (refer to **Figure 1**). For $\rho_{\phi_R,\gamma_R} = \rho_{\phi_Q,\gamma_Q}$ exceeding 0.40, computed ρ_n values are negative and unsafe designs may result if the nominal cross-correlation coefficient is taken as $\rho_n = 0$. Values of ρ_n for all cases are summarized in **Table 3**.

Examples of reliability analysis

Two limit state design examples are presented in this section to demonstrate the quantitative influence of ρ_n on computed reliability index. The first example is the base sliding limit state for a cantilever retaining wall and the second is the pullout limit state for a reinforced soil wall. In the example cases to follow possible correlations between friction angle and unit weight were not considered because the influence of possible correlation between these variables on computed reliability index was found to be negligible. A similar conclusion can be found in **NCHRP (2004)**.

Cantilever wall external sliding limit state

Problem dimensions and nominal (mean) soil property values are given in **Figure 15**. The dimensions are taken from an example that appears in **FHWA (2008)**. The soil properties assumed in this investigation are similar to those that appear in the FHWA design example. Three design scenarios are considered based on assumptions regarding possible correlation between soil properties used for resistance and load terms in the limit state equation (i.e., cross-correlation coefficient between soil property populations in each term is 0 or 1): 1) the backfill and retained soils are the same but the soil friction angle is taken from a different population for the foundation soil; 2) the backfill, retained and foundation soils are all the same; and 3) the retained and foundation soils are the same and both are different from the backfill soil. Note that for the resistance term the soil properties of interest are the friction angle of the foundation soil and the unit weight of the backfill located above the heel. In these calculations (and in the original FHWA example) the virtual wall back is assumed to be frictionless.

Since method bias statistics are not available for load and resistance terms, the analyses were performed assuming the current models are perfectly accurate, i.e., $\mu_{\lambda_R} = \mu_{\lambda_Q} = 1$, $COV_{\lambda_R} = COV_{\lambda_Q} = 0$, and $\rho_R = \rho_Q = 0$. Hence, any uncertainty in analysis outcomes is due to uncertainty in the choice of soil parameters used at design time. Conventional deterministic analysis of external base sliding of the structure using the soil properties in **Figure 15** gave a factor of safety FS = 2.

The results of initial calculation steps are summarized in **Table 4**. The value of $COV_{R_n} = 0.13$ was computed using **Equation 7** and Monte Carlo simulation with lognormally distributed random variables for ϕ described by $\mu_{\phi_R} = \mu_{\phi_Q} = \mu_\phi = 30°$ and $COV_{\phi_R} = COV_{\phi_Q} = COV_\phi = 0.10$, and for γ, $\mu_{\gamma_R} = \mu_{\gamma_Q} = \mu_\gamma = 18$ kN/m^3 and $COV_{\gamma_R} = COV_{\gamma_Q} = COV_\gamma = 0.05$. The COV values for friction angle and unit weight give r = 2. The same statistical values were used to compute COV_{Q_n} using **Equation 8**. For each case identified in **Table 1**, the nominal cross-correlation coefficient ρ_n was computed using MC simulation. These data can be visualized by scatter plots of the type shown in **Figure 9** and can be found in the **Supplemental Materials** to the paper. The values of ρ_n are 0.11, −0.78 and −0.88 for Scenario A (Case 3), Scenario B (Case 2) and Scenario C (Case 5), respectively. The computed reliability index values decrease in the reverse order as $\beta = 4.02$, 2.83 and 2.75. A reasonable target reliability index value for external sliding of this structure when seated on competent ground is $\beta_T = 3.09$ ($P_f = 1/1000$) (**Withiam et al. 1998**). Hence, the structure can be assumed to be unsafe for two of the three scenarios. If nominal correlations between load and resistance terms are ignored, then all three scenarios give $\beta > \beta_T = 3.09$, implying that the structure has an adequate margin of safety against sliding in probabilistic terms. This is an unsafe assessment of margin of safety for two of the example scenarios if nominal load and resistance terms are in fact correlated using the assumed input parameters. For these two cases the difference in terms of probability of failure is more than one order of magnitude. Nevertheless, the practical and easy solution to increase the reliability index for this limit state is to increase the length of the foundation heel.

Reinforcement pullout limit state

Three reinforcing elements are considered: 1) geogrid, 2) steel strip, and 3) soil nail. The pullout limit state for a reinforced soil wall for the geogrid and steel strip cases is based on the Simplified Method recommended by **AASHTO (2014)**. The soil nail calculations are based on methods described by **Watkins and Powell (1992), GEO (2007)** and **FHWA (2015)**. The problem geometry for the geogrid reinforced soil wall case can be referenced to **Figure 8b**. Each wall is H = 10 m high. The other deterministic parameters are assumed as follows: 1) geogrid wall: width of reinforced soil zone, L = 0.7H, S_v = 1.0 m, z = 0.5 m, L_e = 1.5 m and α = 1.07; 2) steel strip wall: L = 0.7H, $S_v = S_h$ = 0.5 m, z = 6 m, L_e = 4.6 m, w = 0.05 m, F = 1.0 and κ = 1.2; 3) soil nail wall: L = 0.9H, $S_v = S_h$ = 1.20 m, D = 0.15 m, z = 6 m, η = 0.75 and L_e = 6.7 m. It should be noted that the depth of the reinforcing element for each structure type was selected to give the minimum factor of safety against pullout failure using the deterministic equations for load and resistance described earlier together with the empirical non-dimensional coefficient values recommended in the references cited above.

For the geogrid and steel strip wall cases, the statistical parameters for soil frictional angle and unit weight are $\mu_{\phi_R} = \mu_{\phi_Q} = \mu_\phi = 30°$ and $COV_{\phi_R} = COV_{\phi_Q} = COV_\phi = 0.10$, and $\mu_{\gamma_R} = \mu_{\gamma_Q} = \mu_\gamma = 18\ kN/m^3$ and $COV_{\gamma_R} = COV_{\gamma_Q} = COV_\gamma = 0.05$. For the soil nail wall case, the mean values were the same as those just reported, but the COV values are $COV_{\phi_R} = COV_{\phi_Q} = COV_\phi = 0.20$ and $COV_{\gamma_R} = COV_{\gamma_Q} = COV_\gamma = 0.10$. This is because soil nails are installed in natural soils while geogrid and steel strip reinforcing elements are installed in engineered soils which are assumed to be less variable. Bias statistics for each pullout analysis type can be found in the references cited in the footnotes to **Table 5**. As before, all random variables are assumed to be lognormally distributed.

The statistics for the spreads in nominal resistance (COV_{R_n}) and nominal load (COV_{Q_n}) were computed in the same manner as that described for the wall example but using the load and resistance equations applicable to each reinforcement type. Scatter plots of R_n and Q_n can be found in the **Supplemental Materials** to this paper. In these examples the computed nominal cross-correlation coefficients varied from 0.39 to −0.70. Computed reliability index values are greater than β_T = 3.09 regardless whether or not nominal correlation was considered. In fact, typical practice for LRFD calibration of the pullout limit state for these systems is to use β_T = 2.33 (P_f = 1/100) (**Allen et al. 2005**). This is because if one element fails there are other reinforcement elements to compensate. The same low reliability index value is assumed for LRFD design of single compression piles that are part of a group of piles which give the foundation system strength redundancy (**Paikowsky et al. 2004**).

As in the cantilever wall case example and the sensitivity analyses presented earlier, nominal correlations between load and resistance values can lead to greater or lower estimates of margins of safety in terms of reliability index or probability of failure. However, for the reinforcement cases analyzed here, the differences do not have a practical impact on design outcomes since the values of β are all greater than 2.33.

It can be noted that margins of safety for this limit state expressed in deterministic or probabilistic frameworks are easily adjusted for other MSE wall examples by changing the values for reinforcement spacing and length which are deterministic. In fact, the prescribed minimum reinforcement length of 0.7H recommended by **AASHTO (2014)** is largely responsible for the large value of β in the example cases here. This empirical constraint is related to the external sliding limit state for these structures. **Huang et al. (2012)** and **Bathurst et al. (2012)** examined the margins of safety against pullout for the most critical layer in a large number of constructed reinforced steel strip and geogrid reinforced soil walls reported in the literature. They concluded that the actual as-built reliability index and factors of safety were well above minimum values recommended in current allowable stress design (ASD) practice and for LRFD calibration, and was attributable to the L = 0.7H minimum length criterion.

Conclusions

This paper is focused on the influence of cross-correlation between nominal load and resistance terms (called nominal correlation for brevity and denoted as ρ_n) on the calculation of reliability index (β) or probability of failure for simple limit states in soil-structure interaction problems. Correlation between nominal load and resistance terms is quantified by the conventional Pearson's cross-correlation coefficient that can vary in the range $-1 \leqslant \rho_n \leqslant +1$. The case with $\rho_n = 0$ corresponds to no correlation and is a tempting assumption for simplicity in reliability-based design and is almost always made for LRFD calibration using readily available reliability theory-based closed-form solutions. A more comprehensive closed-form solution by **Bathurst and Javankhoshdel (2017)** for reliability index (β) is used in the current study. This formulation includes the contribution of possible dependencies between method accuracy (method bias) and nominal values for load and resistance terms. The mean of bias values are used to adjust estimates of factor of safety used at design time to give a more accurate estimate (on average) of the (true) operational factor of safety. The main conclusions drawn from this study are as follows.

1. Nominal load and resistance terms in simple linear limit state equations can be cross-correlated due to the presence of the same random variables in both terms. For design cases with the mean factor of safety within the range of about 1.5 to 3.0, ignoring negative nominal correlations when they are present will typically result in under-estimation of probability of failure by up to two orders of magnitude. On the other hand, ignoring positive nominal correlations when they exist over-estimates probability of failure up to several orders. This error is on the safe side, but the penalty is a more conservative and thus more expensive for design.

2. For limit state functions having the forms examined in this paper for the sliding block problem and reinforcing element pullout problem, the magnitude of nominal correlation is dependent on the ratio of COV of soil friction angle to COV of soil unit weight, and the mean of soil friction angle. Increasing both values was shown to make the computed nominal correlation more negative.

3. The nominal correlation is typically negative when the same soil friction angle appears in both load and resistance terms. The practical implication is that when this is the case, the nominal correlation must be considered to ensure adequate margins of safety for simple limit state designs using closed-form solutions. For cases where load and resistance terms do not share the same soil friction angle, the nominal correlation will always be positive.

4. The nominal correlation has a much stronger influence on computed reliability index when bias dependencies for both load and resistance models are concurrently negative. This is an unfavorable outcome for pullout limit states of reinforcing elements since a survey of load and resistance bias dependencies reported in the literature shows that both are always negative. For bias dependencies with opposite signs or concurrently positive, the influence of nominal correlation is much less.

5. Actual design examples showed that probabilities of failure were at least one order of magnitude different with and without considering nominal correlations. When the probability of failure considering nominal correlation is unsatisfactory, the design may have to be revised to achieve a target minimum acceptable β value even though the conventional factor of safety for the same limit state is satisfactory. This situation highlights the need to treat conventional ASD practice and reliability-based design as two complementary design strategies.

As demonstrated in the paper, the influence of cross-correlation and bias statistics on reliability index can be computed using Monte Carlo simulation techniques directly. However, once the nominal correlation coefficient is computed, the closed-form solution (**Equation 3**) has the advantage of transparency and ease of use (e.g., using Excel spreadsheets). This avoids the complication of practicing engineers having to develop familiarity with Monte Carlo simulation techniques for correlated random parameters and having to carry out a very large number of simulations if the target reliability index is very large.

Finally, it should be noted that the examples that are used here correspond to simple limit states where soil properties occur in both resistance and load model terms in a limit sate function. However, some limit state functions such as the tensile (yield) strength for a soil reinforcing element will not have nominal correlation because the resistance (strength) is unrelated to the surrounding soil properties. Other examples are shallow footings and compression piles when the loads applied to the structure are independent of the soil. For these examples, **Equation 3** is simplified to **Equation 6**.

Acknowledgements

The authors are grateful for financial support through an ENGAGE research grant awarded to the corresponding author by the Natural Sciences and Engineering Research Council of Canada (NSERC).

References

AASHTO. 2014. AASHTO LRFD bridge design specifications, 7th Ed. Washington, DC.

Allen, T.M., and Bathurst, R.J. 2015. Improved simplified method for prediction of loads in reinforced soil walls. Journal of Geotechnical and Geoenvironmental Engineering, 141(11): 04015049.

Allen, T.M., Nowak, A.S., and Bathurst, R.J. 2005. Calibration to Determine Load and Resistance Factors for Geotechnical and Structural Design. Transportation Research Board Circular E-C079, Washington, DC, 93 p.

Ang, A.H., and Tang, W.H. 1984. Probability concepts in engineering planning and design. Vol. 2. Wiley, New York.

Babu, S.G.L., and Singh, V.P. 2011. Reliability-based load and resistance factors for soil-nail walls. Canadian Geotechnical Journal, 48(6): 915−930.

Babu, S.G.L., and Srivastava, A. 2007. Reliability analysis of allowable pressure on shallow foundation using response surface method. Computers and Geotechnics, 34(3): 187−194.

Baecher, G.B., and Christian, J.T. 2003. Reliability and statistics in geotechnical engineering, Wiley, Chichester, UK.

Bathurst, R.J., Allen, T.M., and Nowak, A.S. 2008. Calibration concepts for load and resistance factor design (LRFD) of reinforced soil walls. Canadian Geotechnical Journal, 45(10): 1377–1392.

Bathurst, R.J., Huang, B. and Allen, T.M. 2011. Load and resistance factor design (LRFD) calibration for steel grid reinforced soil walls. Georisk, 5(3-4): 218−228.

Bathurst, R.J., Huang, B. and Allen, T.M. 2012. LRFD calibration of the ultimate pullout limit state for geogrid reinforced soil retaining walls. ASCE International Journal of Geomechanics, Special Issue on Geosynthetics, 12(4): 399–413.

Bathurst, R.J., and Javankhoshdel, S. 2017. Influence of model type, bias and input parameter variability on reliability analysis for simple limit states in soil-structure interaction problems. Georisk, 11(1): 42–54.

Bathurst, R.J., Javankhoshdel, S., and Allen, T.M. 2017. LRFD calibration of simple soil-structure limit states considering method bias and design parameter variability. Journal of Geotechnical and Geoenvironmental Engineering (in press). (http://dx.doi.org/10.1061/(ASCE)GT.1943-5606.0001735).

Burlon, S., Frank, R., Baguelin, F., Habert, J., and Legrand, S. 2014. Model factor for the bearing capacity of piles from pressuremeter test results-Eurocode 7 approach. Géotechnique, 64(7): 513−525.

Chowdhury, R.N., and Xu, D.W. 1993. Rational polynomial technique in slope reliability analysis. Journal of Geotechnical and Geoenvironmental Engineering, 119(12): 1910−1928.

Dithinde, M., Phoon, K.K., De Wet, M., and Retief, J.V. 2011. Characterisation of model uncertainty in the static pile design formula. Journal of Geotechnical and Geoenvironmental Engineering, 137(1): 70−85.

FHWA. 2008. Earth retaining structures – Reference manual. FHWA-NHI-07-071, Federal Highway Administration (FHWA), Washington D.C.

FHWA. 2009. Design and construction of mechanically stabilized earth walls and reinforced soil slopes—Volume I. FHWA-NHI-10-024, FHWA GEC 011-Vol I, Federal Highway Administration (FHWA), Washington D.C.

FHWA. 2015. Geotechnical engineering circular No. 7 soil nail walls—Reference manual. U.S. Department of Transportation Publication No. FHWA-NHI-14-007, Federal Highway Administration, FHWA, Washington, DC.

Geotechnical Engineering Office (GEO). 2007. Good practice in design of steel soil nails for soil cut slopes. GEO technical guidance note No. 23, Hong Kong Government, Hong Kong.

Harr, M.E. 1987. Reliability-based design in civil engineering. New York, NY: McGraw-Hill.

Huang, B., Bathurst, R.J., and Allen, T.M. 2012. LRFD calibration for steel strip reinforced soil walls. Journal of Geotechnical and Geoenvironmental Engineering, 138(8): 922−933.

Huang, B., and Bathurst, R.J. 2009. Evaluation of soil-geogrid pullout models using a statistical approach. Geotechnical Testing Journal, 32(6): 1−16.

International Organization for Standardization. 2015. General principles on reliability of structures. ISO2394:2015, Geneva, Switzerland.

Javankhoshdel, S., and Bathurst, R.J. 2017. Deterministic and probabilistic failure analysis of simple geosynthetic reinforced soil slopes. Geosynthetics International, 24(1): 14−29.

Lacasse, S., and Nadim, F. 1996. Uncertainties in characterizing soil properties. Uncertainty in the Geologic Environment, Madison, ASCE, Reston, VA, 49−75.

Lee, K.L., and Singh, A. 1968. Report of the direct shear comparative study. University of California, Los Angeles, pp. 38.

Lin, P., Bathurst, R.J., Javankhoshdel, S., and Liu, J. 2017a. Statistical analysis of the effective stress method and modifications for prediction of ultimate bond strength of soil nails. Acta Geotechnica, 12(1): 171−182.

Lin, P., Bathurst, R.J., and Liu, J. 2017b. Statistical evaluation of the FHWA simplified method and modifications for predicting soil nail loads. Journal of Geotechnical and Geoenvironmental Engineering, 143(3): 04016107.

Low, B.K., and Tang, W.H. 1997. Probability slope analysis using Janbu's generalized procedure of slices. Computer and Geotechnics, 21(2): 121−142.

Matsuo, M., and Kuroda, K. 1974. Probabilistic approach to design of embankments. Soils and Foundations, 14(2): 1−17.

Melchers, R.E. 1999. Structural reliability analysis and prediction, 2nd Ed. Wiley, Chichester, UK.

Miyata, Y., Bathurst, R.J., and Konami, T. 2011. Evaluation of two anchor plate capacity models for MAW systems. Soils and Foundations, 51(5): 885−895.

Miyata, Y., and Bathurst, R.J. 2012a. Measured and predicted loads in steel strip reinforced c−ϕ soil walls in Japan. Soils and Foundations, 52(1): 1−17.

Miyata, Y., and Bathurst, R.J. 2012b. Analysis and calibration of default steel strip pullout models used in Japan. Soils and Foundations, 52(3): 481−497.

National Cooperative Highway Research Program (NCHRP). 2004. Load and resistance factors for earth pressures on bridge substructures and retaining walls. NCHRP 12-55, Transportation Research Board, National Research Council. Washington, DC, USA.

Nowak, A.S., and Collins, K.R. 2012. Reliability of structures, 2nd Ed. CRC Press, Taylor & Francis Group, Boca Raton, FL.

Paikowsky, S.G. 2010. LRFD design and construction of shallow foundations for highway bridge structures (Vol. 651). Transportation Research Board.

Paikowsky, S.G., Birgisson, B., McVay, M., Nguyen, T., Kuo, C., Baecher, G., Ayyub, B., Stenersen, K., O'Malley, K., Chernauskas, L., and O'Neill, M. 2004. Load and Resistance Factor Design (LRFD) for Deep Foundations. NCHRP Report 507, Transportation Research Board of the National Academies, Washington, DC, Usa, 126 pp.

Parker, C., Simon, A., and Thorne, C.R. 2008. The effects of variability in bank material properties on riverbank stability: Goodwin Greek, Mississippi. Geomorphology, 101(4): 533−543.

Phoon, K.K. 2008. Reliability-based design in geotechnical engineering: computations and applications. Taylor and Francis, London, UK.

Phoon, K.K. 2017. Role of Reliability Calculations in Geotechnical Design. Georisk, 11(1): 4−21.

Phoon, K.K., and Kulhawy, F.H. 1999. Characterization of geotechnical variability. Canadian Geotechnical Journal, 36(4), 612−624.

Phoon, K.K., and Kulhawy, F.H. 2003. Evaluation of Model Uncertainties for Reliability-based Foundation Design. Proceedings, Ninth International Conference on Applications of Statistics and Probability in Civil Engineering, San Francisco, July 6-9 2003, Vol. 2, 1351−1356.

Phoon, K.K., and Kulhawy, F.H. 2005. Characterization of model uncertainties for laterally loaded rigid drilled shafts. Géotechnique, 55(1): 45−54.

PWRC. 2014. Design method, construction manual and specifications for steel strip reinforced retaining walls, 4th Ed., Public Works Research Center, Tsukuba, Ibaraki, Japan. (in Japanese).

Soong, T.T. 2004. Fundamentals of probability and statistics for engineers. Wiley, Chichester, UK.

Stuedlein, A.W., Allen, T.M., Holtz, R.D. and Christopher, B.R. 2011. Assessment of reinforcement strains in very tall mechanically stabilized earth walls. Journal of Geotechnical and Geoenvironmental Engineering, 138(3): 345−356.

Tang, C., and Phoon, K.K. 2017. Model uncertainty of Eurocode 7 approach for bearing capacity of circular footings on dense sand. International Journal of Geomechanics, 17(3): 04016069.

Tang, C., Phoon, K.K., Zhang, L., and Li, D.Q. 2017. Model uncertainty for predicting the bearing capacity of sand overlying clay. International Journal of Geomechanics, 17(7): 04017015.

Watkins, A.T., and Powell, G.E. 1992. Soil nailing to existing slopes as landslip preventive works. Hong Kong Engineer, 20(3): 20−27.

Withiam, J.L., Voytko, E.P., Barker, R.M., Duncan, J.M., Kelly, B.C., Musser, S.C., and Elias, V. 1998. Load and Resistance Factor Design (LRFD) for Highway Bridge Substructures. FHWA HI-98-032, Federal Highway Administration, Washington, DC, USA.

Yu, Y., and Bathurst, R.J. 2015. Analysis of soil-steel bar mat pullout models using a statistical approach. Journal of Geotechnical and Geoenvironmental Engineering, 141(5): 040150.

LIST OF FIGURES

Figure 11. Influence of ratio of COV_ϕ over COV_γ on ρ_n ($\mu_{\phi_R} = \mu_{\phi_Q} = 30°$, $\mu_{\gamma_R} = \mu_{\gamma_Q} = 18$ kN/m^3, $COV_{\phi_R} = COV_{\phi_Q} = COV_\phi$, $COV_{\gamma_R} = COV_{\gamma_Q} = COV_\gamma = 0.05$)

Figure 12. Influence of mean values of friction angle ϕ_R and ϕ_Q on ρ_n ($\mu_{\gamma_R} = \mu_{\gamma_Q} = 18$ kN/m^3, $COV_{\phi_R} = COV_{\phi_Q} = 0.10$, $COV_{\gamma_R} = COV_{\gamma_Q} = 0.05$, $r = 2$)

Figure 13. Influence of mean values of unit weight γ_R and γ_Q on ρ_n ($\mu_{\phi_R} = \mu_{\phi_Q} = 30°$, $COV_{\phi_R} = COV_{\phi_Q} = 0.10$, $COV_{\gamma_R} = COV_{\gamma_Q} = 0.05$, $r = 2$)

Figure 14. Influence of cross-correlation between friction angle and unit weight $\rho_{\phi_R,\gamma_R} = \rho_{\phi_Q,\gamma_Q}$ on ρ_n ($\mu_{\phi_R} = \mu_{\phi_Q} = 30°$, $\mu_{\gamma_R} = \mu_{\gamma_Q} = 18$ kN/m^3, $COV_{\phi_R} = COV_{\phi_Q} = 0.10$, $COV_{\gamma_R} = COV_{\gamma_Q} = 0.05$, $r = 2$)

Figure 15. Cantilever wall example (dimensions from **FHWA (2008)**). Note: Notations in this figure have been selected to match notation conventions in figure source

LIST OF TABLES

Table 1. Cases for computation of cross-correlation coefficient ρ_n between R_n and Q_n

Case	Random variable	
	Friction angle	Unit weight
1	$\phi_R \neq \phi_Q$ or ϕ_Q only [a]	$\gamma_R \neq \gamma_Q$
2	$\phi_R = \phi_Q = \phi$	$\gamma_R = \gamma_Q = \gamma$
3	$\phi_R \neq \phi_Q$	$\gamma_R = \gamma_Q = \gamma$
4	ϕ_Q only [a]	$\gamma_R = \gamma_Q = \gamma$
5	$\phi_R = \phi_Q = \phi$	$\gamma_R \neq \gamma_Q$

Notes: “=” means “same as”; “≠” means “different from”. [a] see **Equation 15b**

Table 2. Ranges of mean and COV values for ϕ_R, ϕ_Q, γ_R and γ_Q for calculation of ρ_n

Random variable	Full range		Typical range	
	Mean	COV	Mean	COV
ϕ_R (°)	10 •50	0.05 •0.30	20 •40	0.10 •0.15
ϕ_Q (°)	10 •50	0.05 •0.30	20 •40	0.10 •0.15
γ_R (kN/m^3)	14 •22	0.05 •0.15	17 •20	0.05 •0.10
γ_Q (kN/m^3)	14 •22	0.05 •0.15	17 •20	0.05 •0.10

Table 3. Summary of ρ_n values for sliding block and pullout limit state sensitivity analysis cases

Case	Cross-correlation coefficient ρ_n between R_n and Q_n				
	Full range [a]		Typical range [a]		Typical value [b]
	Min	Max	Min	Max	
1	0	0	0	0	0
2	−0.94	0.42	−0.88	0.10	−0.70
3	0.01	0.66	0.12	0.54	0.15
4	0.10	0.94	0.19	0.80	0.39
5	−0.97	−0.24	−0.91	−0.44	−0.85

[a] Based on full and typical ranges of mean and COV values for ϕ_R, ϕ_Q, γ_R and γ_Q given in **Table 2**

[b] Based on $\mu_{\phi_R} = \mu_{\phi_Q} = 30°$, $\mu_{\gamma_R} = \mu_{\gamma_Q} = 18$ kN/m^3, $COV_{\phi_R} = COV_{\phi_Q} = 0.10$, $COV_{\gamma_R} = COV_{\gamma_Q} = 0.05$, r = 2

Table 4. Summary of input values and reliability index calculation outcomes for cantilever wall external sliding limit state example (**Figure 15**)

		Scenario A	Scenario B	Scenario C
Resistance model		**Equation 7**	**Equation 7**	**Equation 7**
μ_{λ_R}		1	1	1
COV_{λ_R}		0	0	0
ρ_R		0	0	0
Load model		**Equation 8**	**Equation 8**	**Equation 8**
μ_{λ_Q}		1	1	1
COV_{λ_Q}		0	0	0
ρ_Q		0	0	0
From **Table 1** →		Case 3	Case 2	Case 5
μ_ϕ (°)		30	30	30
μ_γ (kN/m^3)		18	18	18
COV_ϕ		0.10	0.10	0.10
COV_γ		0.05	0.05	0.05
FS		2.0	2.0	2.0
OFS (**Equation 4**)		2.0	2.0	2.0
COV_{R_n}		0.13	0.13	0.13
COV_{Q_n}		0.13	0.13	0.13
ρ_n		0.11	□0.78	□0.88
β	$\rho_n \neq 0$	**4.02 >**	**2.83 <**	**2.75 <**
	$\rho_n = 0$	**3.78**	**3.78**	**3.78**
P_f	$\rho_n \neq 0$	2.9×10^{-5} <	2.3×10^{-3} >	3.0×10^{-3} >
	$\rho_n = 0$	7.8×10^{-5}	7.8×10^{-5}	7.8×10^{-5}

Table 5. Summary of input values and reliability index calculation outcomes for reinforced soil wall pullout limit state examples with three different reinforcement types

		Geogrid [a]	Steel strip [b]	Soil nail [c]
Resistance model		**Equation 9**	**Equation 11**	**Equation 13**
μ_{λ_R}		2.23	1.45	2.98
COV_{λ_R}		0.55	0.39	0.36
ρ_R		−0.46	−0.62	−0.48
Load model		**Equation 10**	**Equation 12**	**Equation 14**
μ_{λ_Q}		0.45	1.12	0.95
COV_{λ_Q}		0.92	0.33	0.38
ρ_Q		−0.36	−0.08	−0.38
From **Table 1** →		Case 2	Case 4	Case 2
μ_ϕ (°)		30	30	30
μ_γ (kN/m^3)		18	18	18
COV_ϕ		0.10	0.10	0.20
COV_γ		0.05	0.05	0.10
FS		2.8	4.6	1.9
OFS (**Equation 4**)		13.9	6.0	6.0
COV_{R_n}		0.13	0.05	0.28
COV_{Q_n}		0.13	0.13	0.25
ρ_n		−0.70	0.39	−0.70
β	$\rho_n \neq 0$	**3.18 <**	**3.73 >**	**3.16 <**
	$\rho_n = 0$	**3.23**	**3.69**	**3.82**
P_f	$\rho_n \neq 0$	7.4×10^{-4} >	9.6×10^{-5} <	7.9×10^{-4} >
	$\rho_n = 0$	6.2×10^{-4}	1.1×10^{-4}	6.7×10^{-5}

Notes: [a] Bias statistics from **Allen and Bathurst (2015)**, **Huang et al. (2012)**
[b] Bias statistics from **Miyata and Bathurst (2012b)**, **Huang and Bathurst (2009)**
[c] Bias statistics from **Lin et al. (2017a, b)**

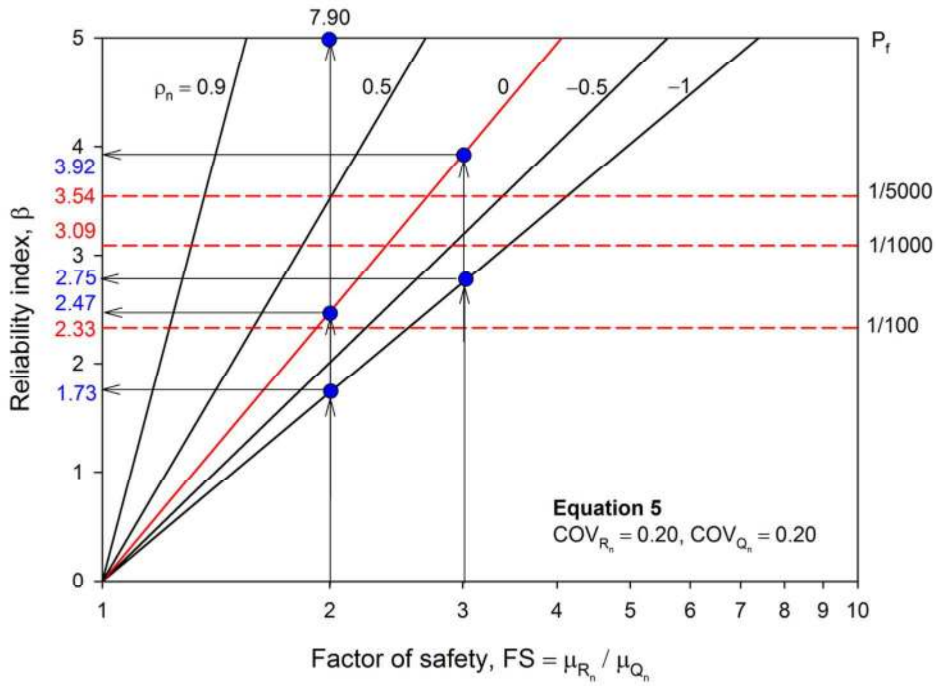

Fig1

121x88mm (300 x 300 DPI)

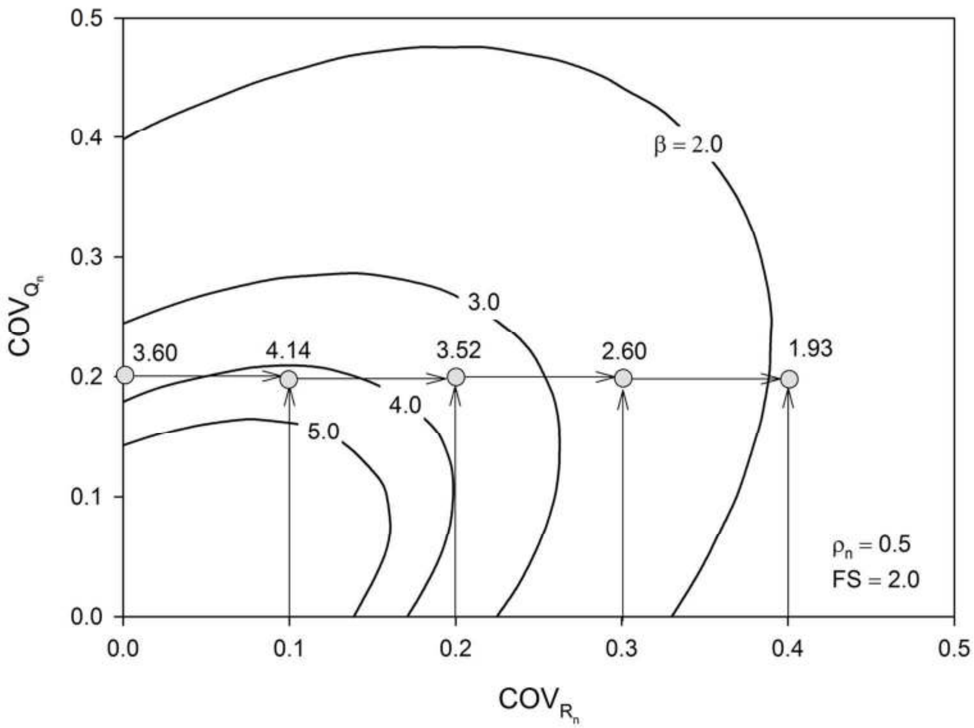

Fig2

120x97mm (300 x 300 DPI)

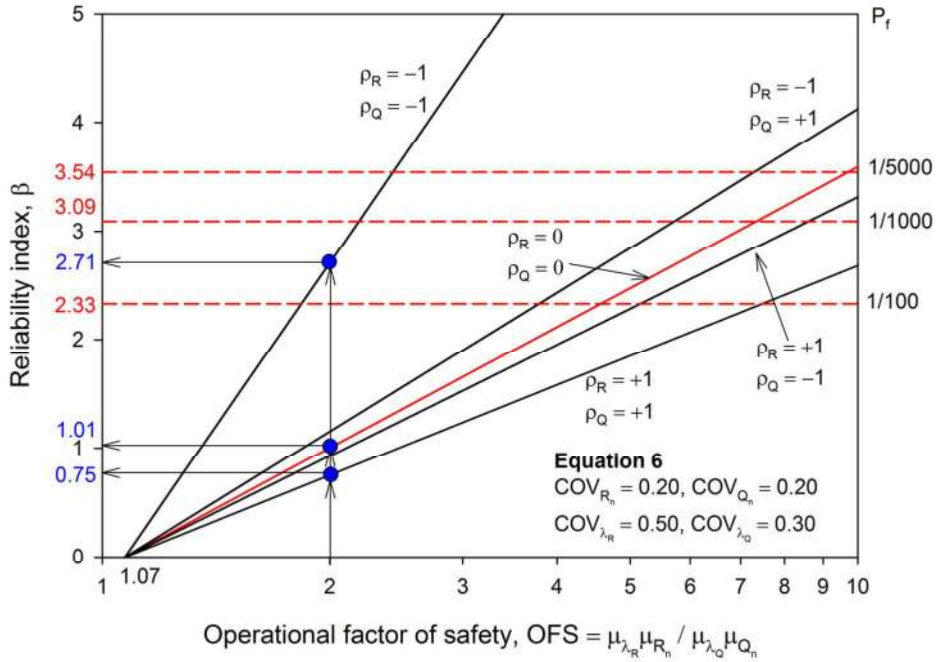

Fig3

121x88mm (300 x 300 DPI)

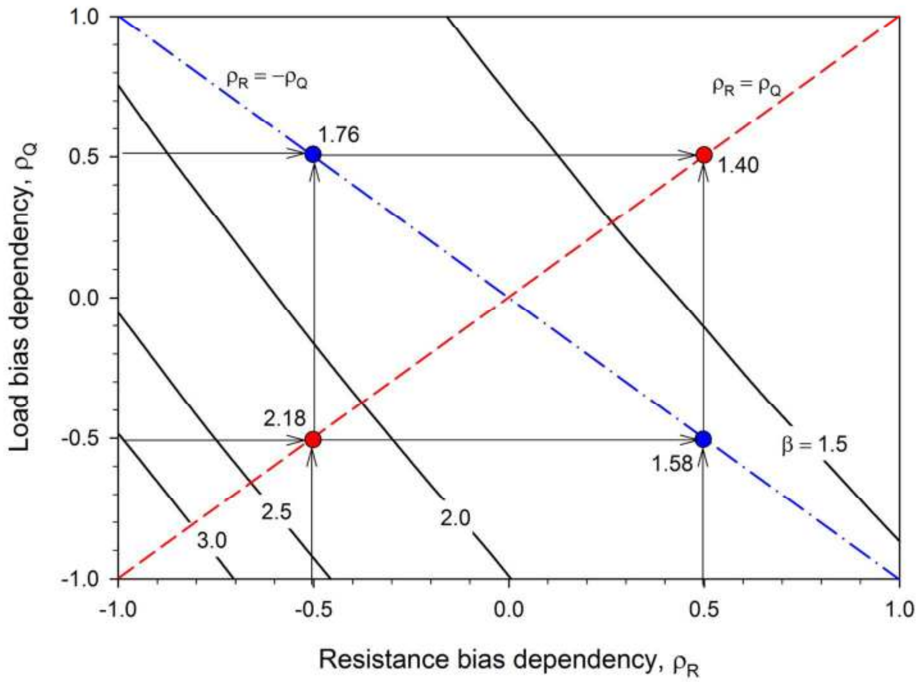

Fig4

120x90mm (300 x 300 DPI)

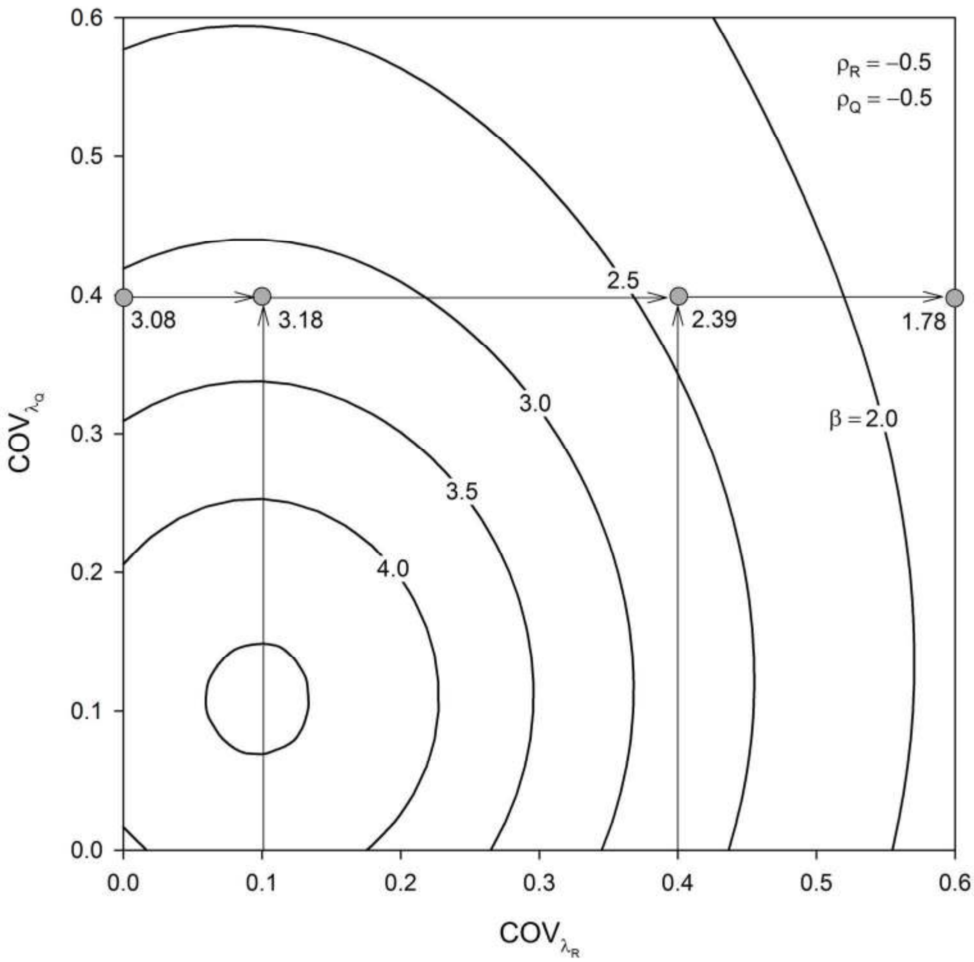

Fig5

155x161mm (300 x 300 DPI)

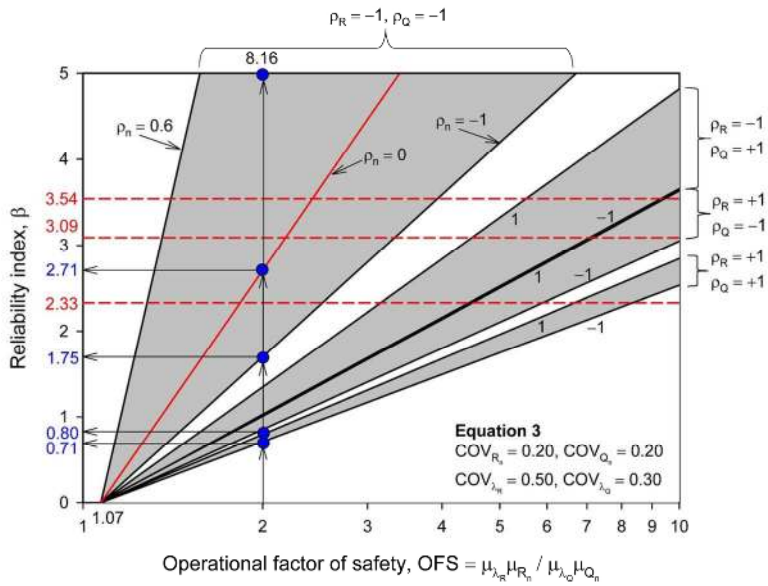

Fig6

143x97mm (300 x 300 DPI)

(a)

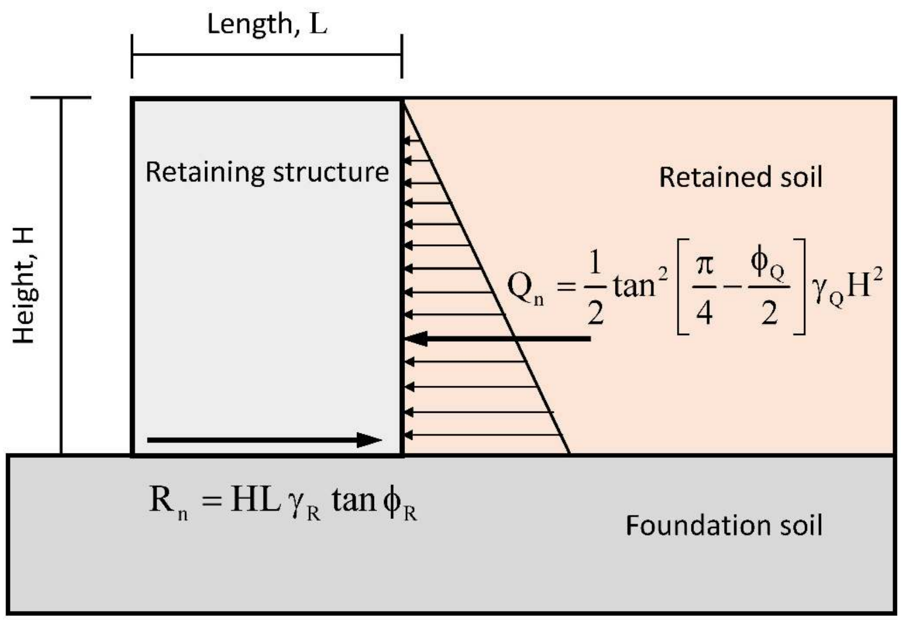

Length, L
Height, H
Retaining structure
Retained soil
$Q_n = \frac{1}{2}\tan^2\left[\frac{\pi}{4} - \frac{\phi_Q}{2}\right]\gamma_Q H^2$
$R_n = HL\,\gamma_R \tan\phi_R$
Foundation soil

(b)

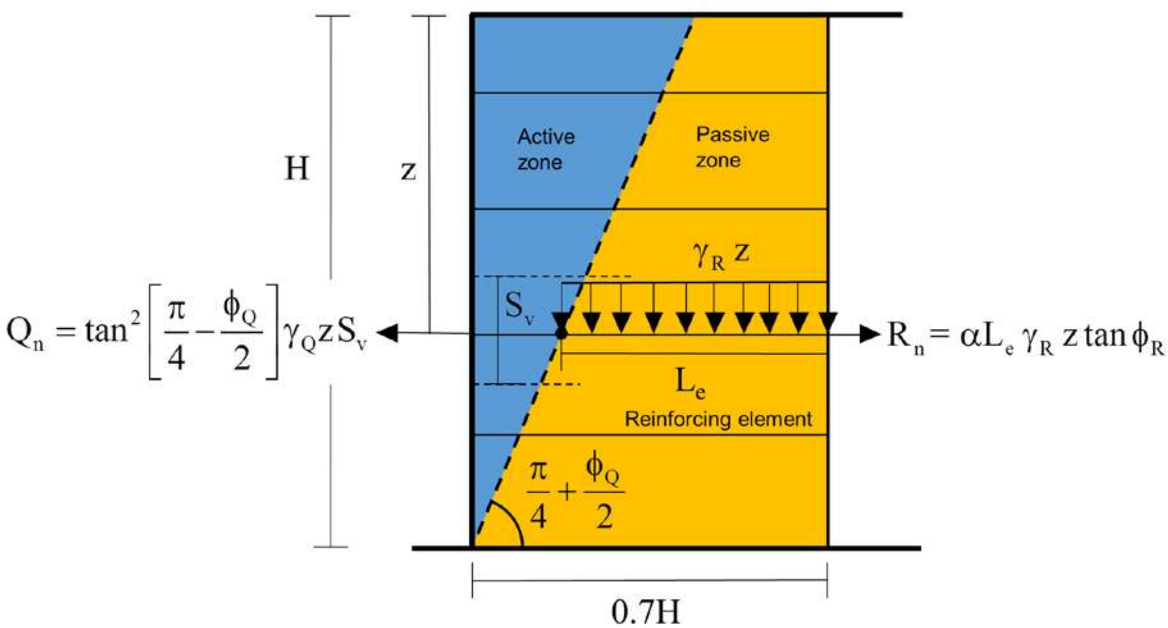

H
z
Active zone
Passive zone
$\gamma_R\, z$
S_v
$Q_n = \tan^2\left[\frac{\pi}{4} - \frac{\phi_Q}{2}\right]\gamma_Q z S_v$
$R_n = \alpha L_e\, \gamma_R\, z \tan\phi_R$
L_e
Reinforcing element
$\frac{\pi}{4} + \frac{\phi_Q}{2}$
0.7H

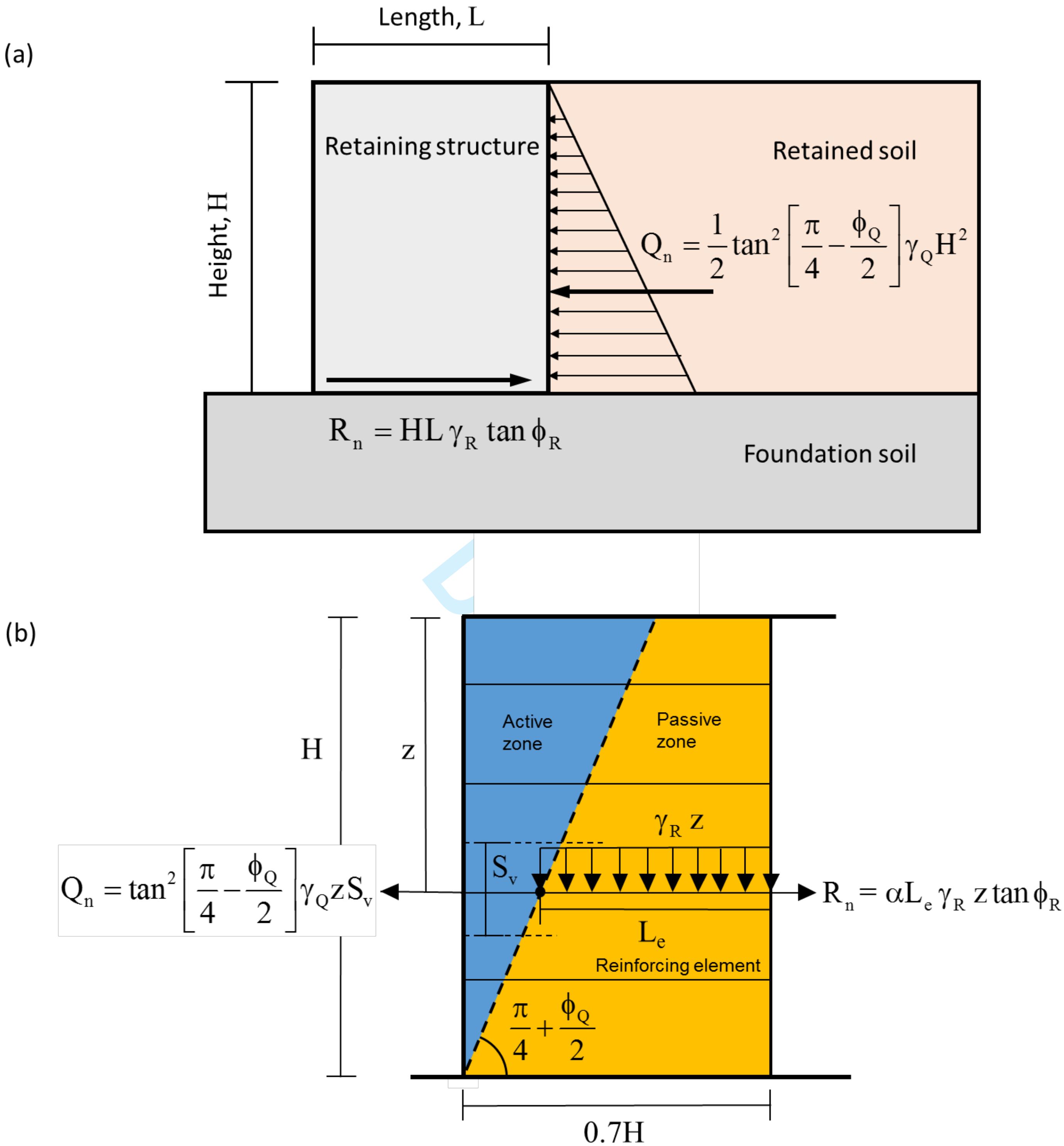
(a)
Length, L
Height, H
Retaining structure
Retained soil
$Q_n = \frac{1}{2}\tan^2\left[\frac{\pi}{4} - \frac{\phi_Q}{2}\right]\gamma_Q H^2$
$R_n = HL\,\gamma_R \tan\phi_R$
Foundation soil
(b)
H
z
Active zone
Passive zone
$\gamma_R\, z$
S_v
$Q_n = \tan^2\left[\frac{\pi}{4} - \frac{\phi_Q}{2}\right]\gamma_Q z S_v$
$R_n = \alpha L_e \gamma_R\, z \tan\phi_R$
L_e
Reinforcing element
$\frac{\pi}{4} + \frac{\phi_Q}{2}$
0.7H

(a)

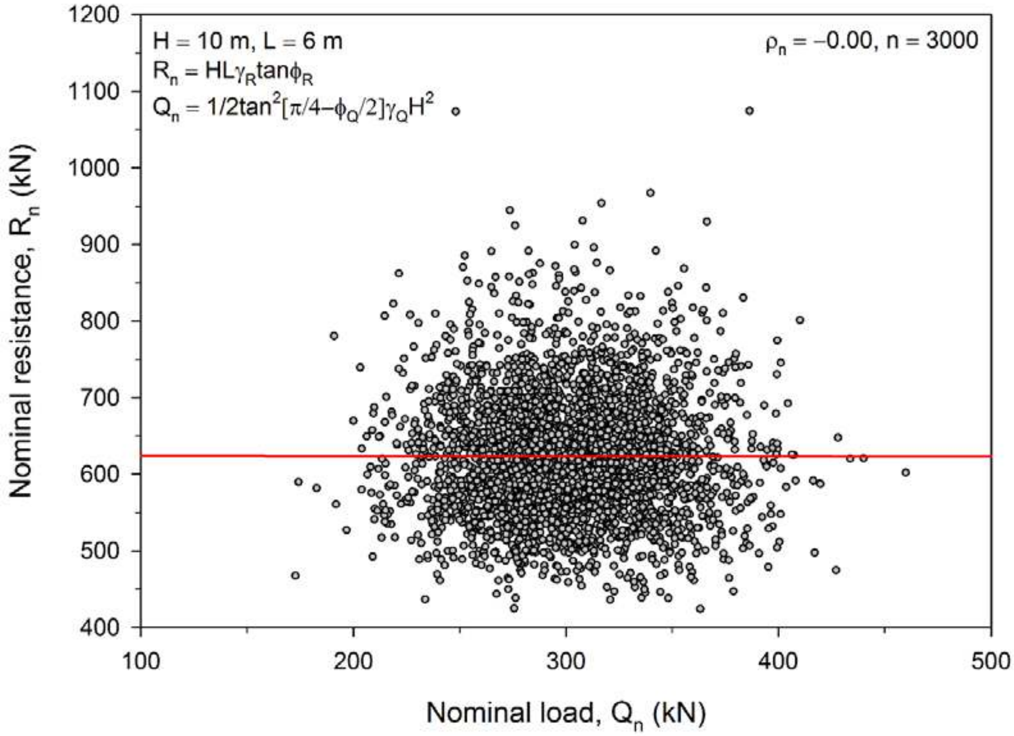
H = 10 m, L = 6 m
$R_n = HL\gamma_R\tan\phi_R$
$Q_n = 1/2\tan^2[\pi/4-\phi_Q/2]\gamma_Q H^2$
$\rho_n = -0.00$, n = 3000
Nominal resistance, R_n (kN)
Nominal load, Q_n (kN)
400
500
600
700
800
900
1000
1100
1200
100
200
300
400
500

(b)

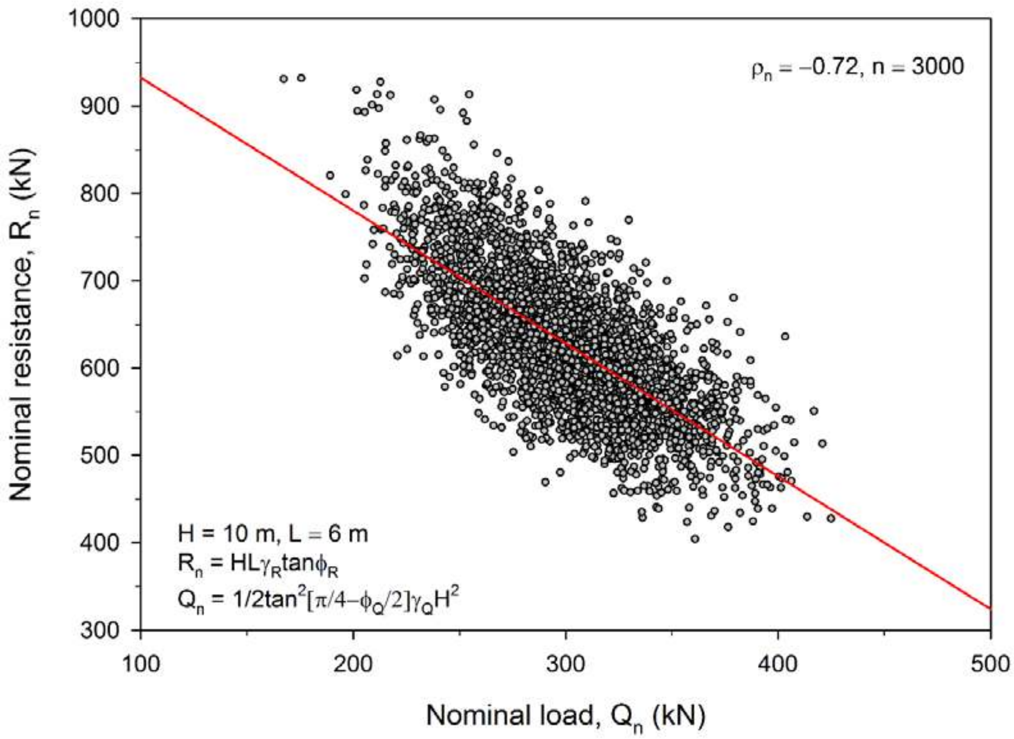
$\rho_n = -0.72$, n = 3000
H = 10 m, L = 6 m
$R_n = HL\gamma_R\tan\phi_R$
$Q_n = 1/2\tan^2[\pi/4-\phi_Q/2]\gamma_Q H^2$
Nominal resistance, R_n (kN)
Nominal load, Q_n (kN)
300
400
500
600
700
800
900
1000
100
200
300
400
500

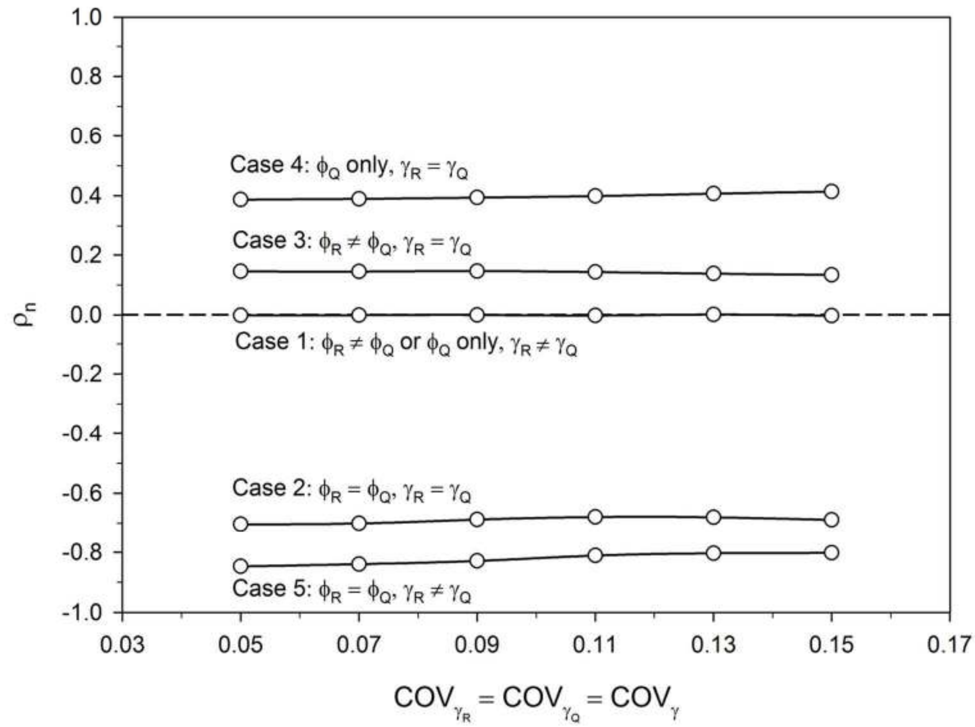

Fig10

121x97mm (300 x 300 DPI)

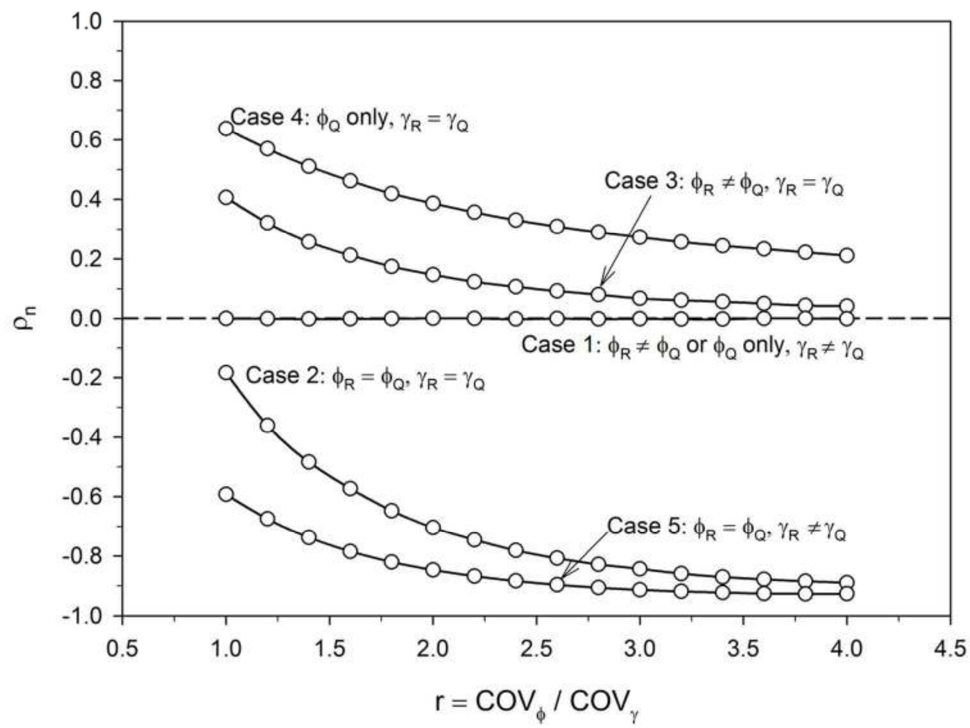

Fig11

120x95mm (300 x 300 DPI)

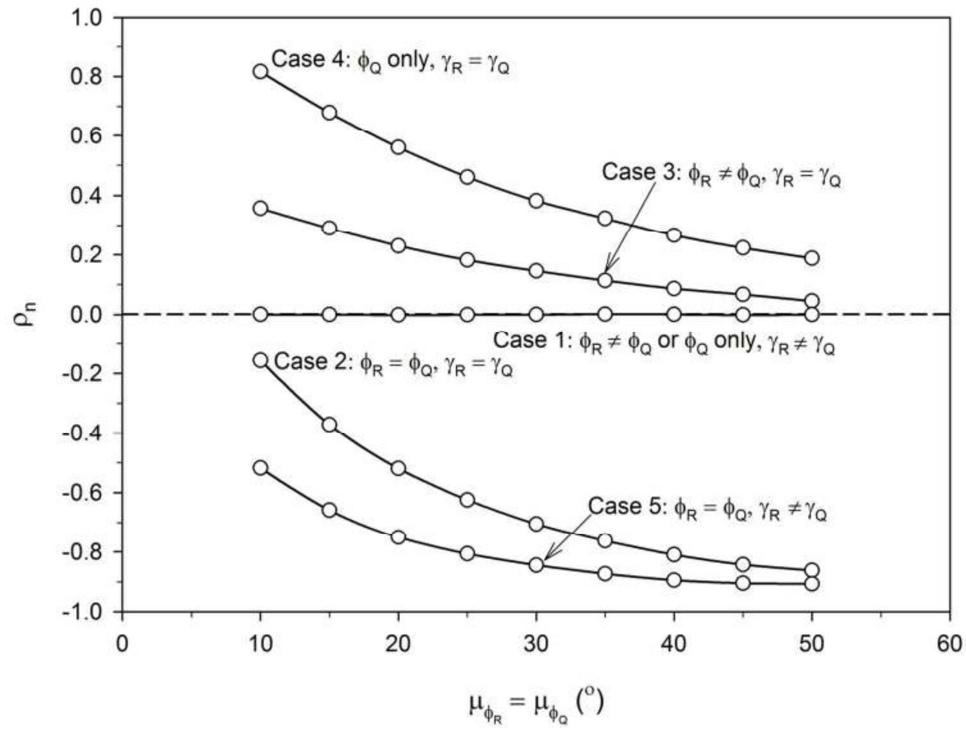

Fig12

121x97mm (300 x 300 DPI)

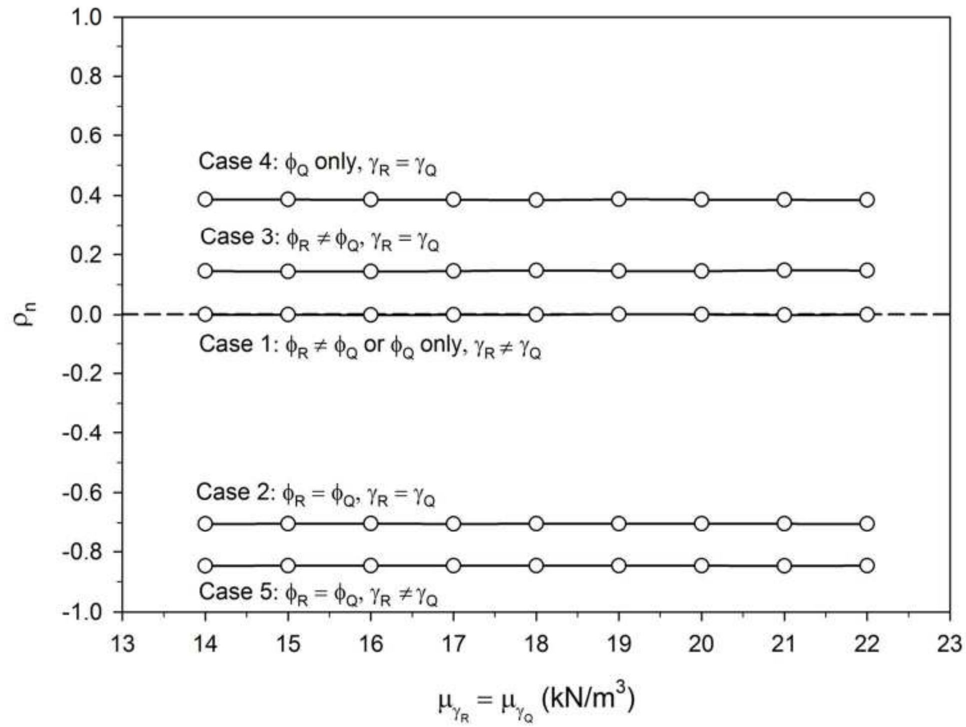

Fig13

121x97mm (300 x 300 DPI)

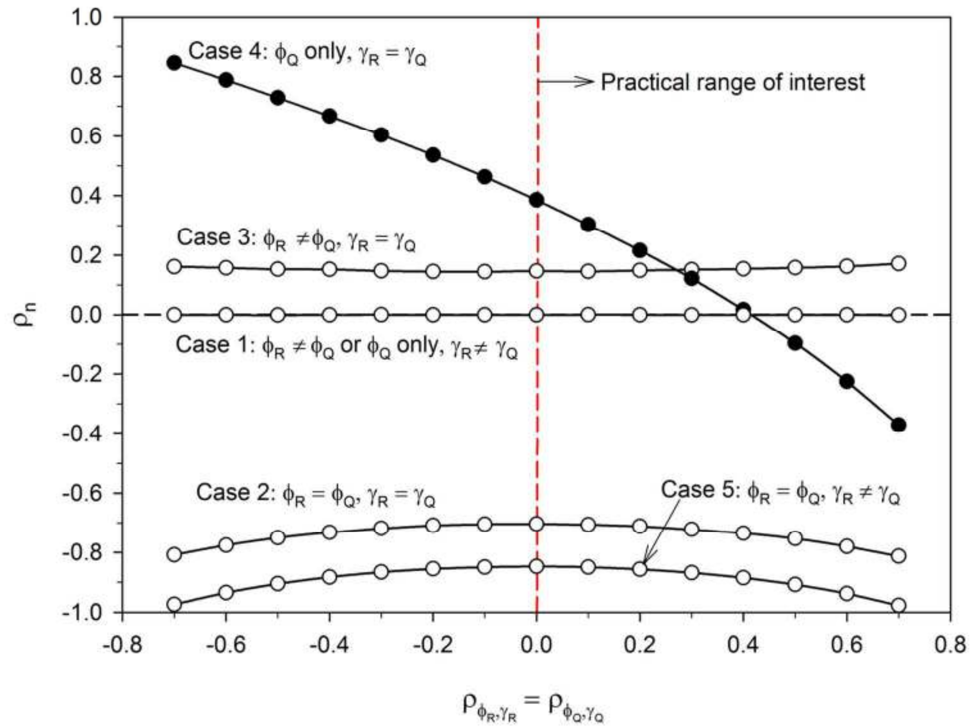

Fig14

121x97mm (300 x 300 DPI)

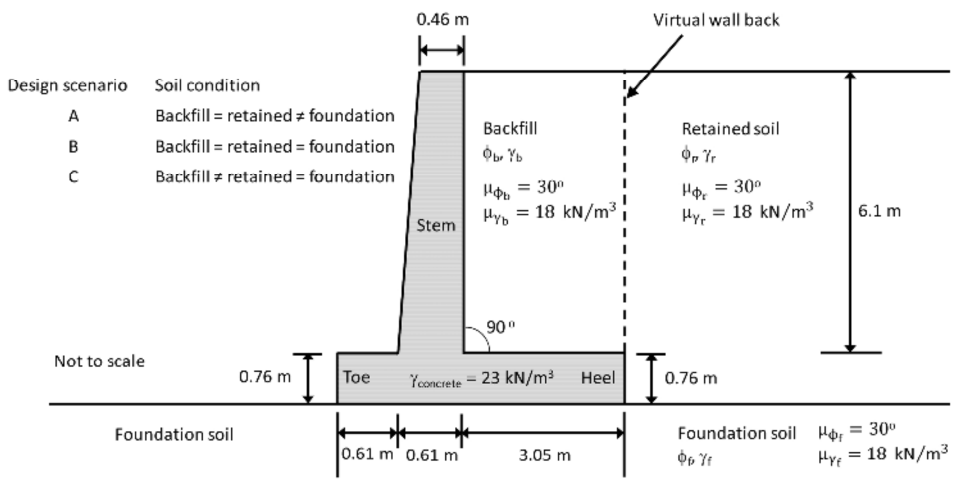

Fig15

190x107mm (300 x 300 DPI)